# Quantum criticality in Ising chains with random hyperuniform couplings

P. J. D. Crowley,[1] C. R. Laumann,[1] and S. Gopalakrishnan[2,3]
[1]*Physics Department, Boston University, Boston, Massachusetts 02215, USA*
[2]*Department of Physics and Astronomy, CUNY College of Staten Island, Staten Island, New York 10314, USA*
[3]*Physics Program and Initiative for the Theoretical Sciences, The Graduate Center, CUNY, New York, New York 10016, USA*

(Received 7 February 2019; revised manuscript received 2 October 2019; published 17 October 2019)

We study quantum phase transitions in transverse-field Ising spin chains in which the couplings are random but hyperuniform, in the sense that their large-scale fluctuations are suppressed. We construct a one-parameter family of disorder models in which long-wavelength fluctuations are increasingly suppressed as a parameter $\alpha$ is tuned. For $\alpha = 0$, one recovers the familiar infinite-randomness critical point. For $0 < \alpha < 1$, we find a line of infinite-randomness critical points with continuously varying critical exponents; however, the Griffiths phases that flank the critical point at $\alpha = 0$ are absent at any $\alpha > 0$. When $\alpha > 1$, randomness is a dangerously irrelevant perturbation at the clean Ising critical point, leading to a state we call the critical Ising insulator. In this state, thermodynamics and equilibrium correlation functions behave as in the clean system. However, all finite-energy excitations are localized, thermal transport vanishes, and autocorrelation functions remain finite in the long-time limit. We characterize this line of hyperuniform critical points using a combination of perturbation theory, renormalization-group methods, and exact diagonalization.

DOI: 10.1103/PhysRevB.100.134206

## I. INTRODUCTION

Quenched randomness has profound effects on the thermodynamics and dynamics of quantum systems. Equilibrium quantum critical points are unstable to weak randomness if the correlation length exponent violates the Harris criterion $\nu > 2/d$, where $d$ is the spatial dimension [1]. When the clean critical point is unstable, the system might exhibit a random critical point [2], at which its properties are heterogeneous on all length scales, or the phase transition might be rounded [3] or preempted, for instance, rare-region effects might destabilize one of the phases (for recent examples, see Refs. [4,5]). In addition, disorder qualitatively modifies quantum dynamics through Anderson localization of elementary excitations [6]. In low-dimensional systems, the Harris bounds are particularly stringent and, besides, weak randomness localizes all excitations [6]. Thus, at clean low-dimensional quantum critical points, both equilibrium properties and dynamics tend to be unstable to weak randomness. In the paradigmatic instance of the transverse-field Ising chain [7], the clean correlation length exponent $\nu = 1$, which violates the Harris criterion; for any disorder, the true critical point is at infinite randomness [8–10], and all excitations at nonzero energy are exponentially localized.

This standard analysis applies when the disorder lacks large-scale spatial correlations. However, localization and the instability of clean critical points occur more generally, even for deterministic quasiperiodic potentials [11–23]. Quasiperiodic couplings, when weak, neither affect critical properties nor localize excitations; thus, unlike random couplings, they are perturbatively irrelevant for both statics and dynamics. At a critical strength of the quasiperiodic potential, however, all excitations localize and the equilibrium critical point is concomitantly destabilized [24–27]. That the onset of localization and the critical-point instability coincide in both random and quasiperiodic systems might suggest that they are somehow fundamentally linked; this is consistent with the intuition [28] that statics and dynamics are inherently linked at quantum phase transitions. Conceptually, however, localization and the instability of critical points stem from different aspects of disorder: the former is due to the disorder potential having a continuous momentum-space spectrum, the latter, to long-wavelength fluctuations. Uncorrelated randomness has both features, while quasiperiodic potentials have neither. However, a broad class of *random* patterns also have suppressed large-scale fluctuations. These patterns are called "hyperuniform" [29–32]. The local value of the order parameter $\delta_i$ at site $i$ in disordered system is characterized by its spatial average $\delta = [\delta_i]$ and with fluctuation scale set by the standard deviation $\sigma(\delta_i)$. Consider the integrated value $S_l(i) = \sum_{|j|<l} \delta_{i+j}$ summed over the region of linear size $l$ in $d$ dimensions and centered at site $i$ is characterized by an asymptotic mean $[S_l] \sim l^d \delta$. $S_l(i)$ For short-range correlated $\delta_i$, the fluctuations $\sigma(S_l)$ are Poissonian, scaling as $\sigma(S_l) \sim l^{d/2}$. The spatial variation of $\delta_i$ is said to be hyperuniform if the fluctuations scale as $\sigma(S_l) \sim l^\beta$ with $\beta < d/2$. Even in maximally uniform structures, such as crystals, where $\delta_i$ has the periodicity of the lattice, there are still fluctuations of order $\sigma(S_l) \sim l^{(d-1)/2}$; in a period structure this contribution comes from the boundary. We shall refer to systems with $\beta = (d-1)/2$ as *strongly hyperuniform* (class I of Ref. [32]). Systems with intermediate exponent $(d-1)/2 < \beta < d/2$ are *weakly hyperuniform* (classes II and III of Ref. [32]).

This work considers quantum phase transitions in which the control parameter is spatially varying and exhibits random hyperuniform fluctuations. Previous analyses have extensively explored the implications of hyperuniform fluctuations in particle density, both theoretically and experimentally in

 ©2019 American Physical Society

photonic materials [33,34], and their localization properties have been studied numerically [35]; however, phase transitions in systems with hyperuniform couplings have not previously been explored. We focus on the transverse-field Ising model, subject to random hyperuniform bonds and/or transverse fields, with tunable extent of hyperuniformity; the picture that emerges from our study is quite general, however, and applies to a range of phase transitions in systems with hyperuniform couplings. The models we introduce are constructed in momentum space, and are thus simple to implement in ultracold atomic gases using spatial light modulators [36] or in "quantum gas microscope" experiments [37]. The hyperuniform couplings in the models we consider lead to a modification to the usual Harris criterion, which is obtained for uncorrelated spatial disorder. This alters the condition for the relevance of the disorder to the critical properties of the transition. Despite this change, as we consider one-dimensional models with local hopping subject to random bonds with continuous Fourier spectra, the $E \neq 0$ excitations remain subject to weak localization. Thus, these models are intermediate between random and quasiperiodic systems: all excitations localize at weak disorder, but the clean critical points need not be unstable. Hyperuniform disorder comes about due to correlations. The effect of correlated disorder on localization [38–40] and phase transitions [41–44] have been previously explored; these works, however, were concerned with the case of locally *correlated* disorder, whereas this work addresses local *anticorrelations*, which naturally give rise to entirely different physics.

We explore the critical point (and near-critical phases) of the random hyperuniform transverse-field Ising model (TFIM) as a function of a parameter $\alpha$, defined in Sec. II, that tunes the degree of hyperuniformity (Fig. 1); $\alpha$ is related to the wandering exponent $\beta$ via $\beta = \max\{0, (1-\alpha)/2\}$. Our results are as follows. For strongly hyperuniform systems, disorder is irrelevant at the clean critical point, and (to leading order) does not affect thermodynamics or equal-time correlation functions. It is counterintuitive that the disorder localize excitations, but remain irrelevant to critical properties; this is possible as the localization length diverges faster than the clean correlation length (Fig. 2) at low energies [or, equivalently, under a renormalization-group (RG) flow]. However, despite irrelevance, the dynamics is completely altered even for weak disorder: thermal transport vanishes, and autocorrelation functions do not decay to zero; a wave packet has a ballistically moving front that remains well defined at all times (a remnant of the $z = 1$ clean critical dynamics), but the front attenuates as it moves, and at late times the weight at the front shrinks to zero (Fig. 2). We call the resulting unconventional critical point the "critical Ising insulator" (CII); because disorder acts as a dangerous irrelevant variable here, we are able to develop an essentially complete analytic understanding of the unusual dynamics on this critical line.

In the weakly hyperuniform case, disorder is relevant, and we find a line of infinite-randomness critical points with continuously varying critical exponents (Fig. 3). Unlike the uncorrelated $\alpha = 0$ case, there are no Griffiths phases for any degree of hyperuniformity; we explain this with an elementary counting argument. We explore these critical points via strong-disorder renormalization-group (SDRG) methods.

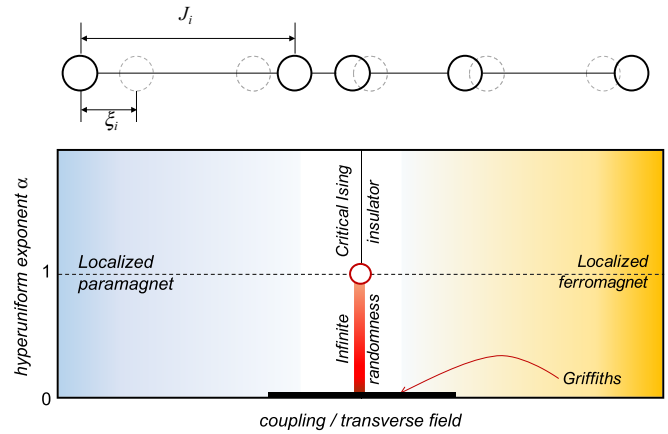


FIG. 1. Upper panel: simple model with strongly hyperuniform ($\alpha = 2$) bond randomness. Each *site* is displaced by an independent random amount $\xi_i$ from its equilibrium position; this leads to bonds $J_i$ that are evidently strongly hyperuniform, in the sense that the variance of $\sum_{i=1}^{l} J_i$ tends to a constant independent of $l$. Lower panel: phase diagram of the random hyperuniform TFIM. Away from criticality, all excitations are localized for any randomness; however, the universality class of the critical point changes as the hyperuniformity parameter $\alpha$ is varied. A line of infinite-randomness critical points, with continuously varying exponents, terminates at a multicritical point, beyond which disorder is dangerously irrelevant (the critical Ising insulator).

Our SDRG results for the average spin correlations at the critical point yield unexpected nonmonotonic behavior: these correlations go as $[\langle \tau_i^x \tau_{i+l}^x \rangle] \sim l^{-2\Delta_\sigma}$, where the exponent $\Delta_\sigma$ first *increases* as the model is made more hyperuniform, then drops discontinuously. We attribute this effect to rare regions (which dominate response in the conventional random TFIM)

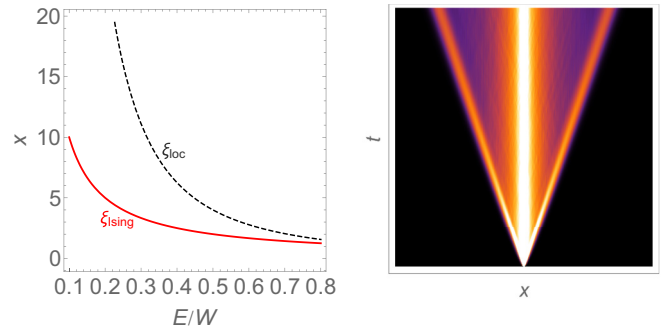


FIG. 2. Critical length scales and dynamics in the strongly hyperuniform Ising model. Left: the length-energy scaling of two relevant scales at the Ising critical point: the clean correlation length $\xi_{\text{clean}} \sim 1/|E|$ and the localization length $\xi_{\text{loc}} \sim 1/|E|^{\alpha}$. When $\alpha > 1$ the localization length diverges faster, so it appears asymptotically larger than the correlation length in the low-energy critical properties. The critical properties are then controlled by the clean Ising correlation length. Right: expansion of an initially localized wave packet along the CII line at $\alpha = 2$. The bulk of the wave packet is localized (corresponding to high-energy components of the wave packet), but there is a rapidly attenuating component that propagates at the light cone, depositing weight as it goes.

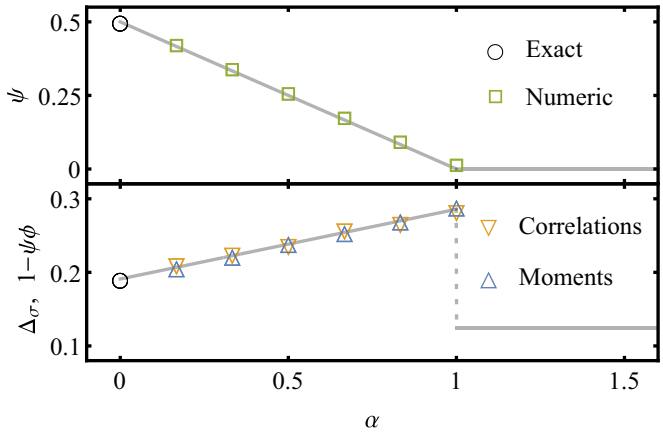


FIG. 3. Weakly hyperuniform systems. Critical exponents at the Ising transition vs hyperuniformity parameter $\alpha$, extracted from the strong-disorder renormalization group. Upper panel shows the length-time scaling $\log t \sim l^{\psi}$, with the analytically exact results for $\alpha = 0$ [8] in agreement with the numerical results for $0 < \alpha \leqslant 1$. Lower panel plots the *average* order parameter scaling dimension $[\langle \tau_i^x \tau_{i+l}^x \rangle] \sim l^{-2\Delta_\sigma}$, extracted from the correlations, and the scaling of the magnetic moment $\mu_l \sim l^{\psi\phi}$. The relation $\Delta_\sigma = 1 - \psi\phi$ is seen to hold.

getting progressively less dominant, and eventually becoming subleading to typical regions.

The rest of this work is organized as follows. In Sec. II we introduce a family of Ising models with random hyperuniform couplings. In Sec. III we use perturbative stability arguments, as well as exact results for the zero-mode wave function, to identify the perturbative (strongly hyperuniform) and nonperturbative (weakly hyperuniform) regimes. (In the process, we also generalize the Harris criterion to the hyperuniform case.) We then explore the equilibrium and dynamical properties of the strongly hyperuniform critical point (Sec. IV) and the weakly hyperuniform critical point (Sec. V), using a combination of perturbative and strong-randomness methods. In Sec. VI we present numerical results, from exact diagonalization, on the evolution of correlation functions as the degree of hyperuniformity is changed. Finally, in Sec. VII we summarize our results and address their implications for more general phase transitions in hyperuniform systems.

## II. MODELS AND REALIZATIONS

We consider the transverse-field Ising model (TFIM) with spatially varying couplings:

$$H = \frac{1}{2} \sum_{i=1}^{L} \left( h_i \tau_i^z + J_i \tau_i^x \tau_{i+1}^x \right), \tag{1}$$

where $\tau^\alpha$ are the Pauli matrices. We construct the coefficients $h_i, J_i$ as follows. For concreteness, consider the $J_i$; we choose $J_i$ to have the form $J_i \equiv J_0 \exp(-s q_i)$, where $q_j \equiv \frac{1}{\sqrt{L}} \sum_k q_k e^{-ikj}$ (with $k = 2\pi n/L$, and $n = 1 \ldots L$), and $q_k$ are random numbers with correlations given by the structure factor $S_\alpha(k, k')$:

$$S_\alpha(k, k') \equiv [q_k q_{-k'}] \sim |k|^\alpha \delta_{kk'}, \tag{2}$$

where from here on $[\cdot]$ denotes disorder averaging. In numerics we use $q_k = |\sin(k/2)|^{\alpha/2} \frac{1}{\sqrt{L}} \sum_j \xi_j e^{ikj}$ $(j = 1 \ldots L)$ for independently identically distributed (iid) $\xi_j$ drawn from the uniform distribution of mean $[\xi_j] = 0$ and unit variance $[\xi_j^2] = 1$. For this choice of $q_k$ one finds $[q_k q_{-k'}] = |\sin(k/2)|^\alpha \delta_{kk'} \sim |k|^\alpha \delta_{kk'}$ as required.

When $s$ is small, we can expand $J_i$ to linear order in $q_i$, so that both have the same fluctuation properties; for the nature of the critical point, however, it is the distribution of $\ln J_i$ that we would like to be hyperuniform (Sec. III B). It is known [30] that when $0 < \alpha < 1$, the fluctuations scale as $\sigma(\sum_{i=1}^{l} q_i) \sim l^{(1-\alpha)/2}$, where $\sigma(\cdot)$ denotes the standard deviation; for $\alpha > 1$, the system is strongly hyperuniform since these fluctuations are independent of the size of the region. Models with general $\alpha$ involve long-range correlations of the disordered couplings, as a result of their nonanalytic behavior as $k \to 0$. For the bulk of our analysis and numerical work we fix $h_i$ to have the same distribution as $J_i$ in order to retain the standard self-duality properties of the Ising model. However, we have checked that our results are unaffected if, instead, we choose either $h_i$ or $J_i$ to be constant, so long as at least one of the terms is random and hyperuniform.

Since these patterns (2) have simple properties in Fourier space, they can in principle be implemented in systems of ultracold atoms using spatial light modulators (which engineer potentials in $k$ space [45,46]). Spatial light modulators would allow one to realize hyperuniform couplings in, e.g., Rydberg-atom arrays, in which the TFIM has been realized [47,48]. Also, in realizations of the TFIM that use quantum gas microscopes [37], all parameters can be addressed and tuned locally. Beyond ultracold gases, random hyperuniform couplings can also be straightforwardly realized in arrays of magnetic adatoms [49], deposited precisely on surfaces using scanning-tunneling microscopy, which can be chosen to have random hyperuniform spacings.

For the specific case $\alpha = 2$, the structure factor is analytic at $k = 0$ so a simple local construction of the random potential for this case exists [50] (Fig. 1, upper panel). Define $q_j = j + \xi_j$, where $\xi_j$ are iid random "displacements" with a mean $[\xi_j] = 0$. Then, $J_j = J \exp(s\{q_j - q_{j-1}\})$. This choice of couplings is physically natural: it corresponds to exponentially decaying spin-spin interactions between spins on sites that are randomly displaced from equilibrium positions on a regular crystalline lattice. One can check that for weak variations in $J_i$, we have $S_\alpha(k, k') = \delta_{kk'} [\xi^2] \sin^2(k/2) \sim \delta_{kk'} k^2$; thus, this model is indeed hyperuniform with $\alpha = 2$. Other hyperuniformity exponents $\alpha$ may be realized in a similar manner if the spin degrees of freedom are spaced such that the fluctuations on the number of spins in a given volume are hyperuniform. Such models may arise naturally for judiciously chosen processes [51,52].

We note that the TFIM with arbitrary couplings can be mapped via Jordan-Wigner transformation to a model of free Majorana fermions with spatially varying hopping. Specifically [25–27],

$$H = \frac{i}{2} \sum_i \left( J_i \gamma_{2i} \gamma_{2i+1} + h_i \gamma_{2i+1} \gamma_{2i+2} \right), \tag{3}$$

where the Majorana operators are related to the spins via the relations

$$\gamma_{2i} \equiv \left(\prod_{j<i} \tau_j^z\right) \tau_i^x; \quad \gamma_{2i+1} \equiv \left(\prod_{j<i} \tau_j^z\right) \tau_i^y. \tag{4}$$

This free-fermion representation allows for $H$ to be brought to a diagonal form $H = i \sum_n E_n \eta_{2n} \eta_{2n+1}$ using exact diagonalization, and thus permits studies of relatively large systems.

## III. CRITICAL POINTS AND PHASES VS $\alpha$

In this section we identify the various regimes of behavior as a function of the hyperuniformity parameter $\alpha$, using perturbative arguments and the exact solution for the zero mode of the Ising model. This leads us to separate the phase diagram into a regime where disorder is perturbatively irrelevant [i.e., for strongly hyperuniform couplings (Sec. IV)] and a regime where it is relevant [i.e., for weakly hyperuniform couplings (Sec. V)]. In subsequent sections we address these regimes separately, using the methods appropriate to each.

### A. Harris criterion

As a first step to understanding the relevance of hyperuniformity, we generalize the Harris criterion to random hyperuniform potentials in one dimension. The argument below generalizes that given by Luck [53] for quasiperiodic potentials.

The control parameter $\delta = [\log h_i - \log J_i]$ describes the deviation of a thermodynamic system from criticality. Analogously, one can define a local control parameter $\delta_l$, which describes the deviation from criticality within a finite region of size $l$. The value of $\delta_l$ depends on the disorder realization (or equivalently the choice of finite region); $\delta_l$ has mean value $[\delta_l] = \delta$, and fluctuations given by the corresponding standard deviation $\sigma(\delta_l)$.

In the strongly hyperuniform case, the fluctuations of $\delta_\xi$ within a region of the size of the correlation length $\xi$ are of scale $\sigma(\delta_\xi) \sim 1/\xi \sim \delta^\nu$. For the clean criticality to be stable, we require that $[\delta_\xi] > \sigma(\delta_\xi)$, i.e., $\delta > \delta^\nu$, as the critical point is approached ($\delta \to 0$). In this case, stability of the clean universality to hyperuniform disorder requires $\nu \geqslant 1$. Thus, the stability of the clean TFIM critical point in one dimension (where $\nu = 1$) is marginal. For weakly hyperuniform systems, the fluctuations are of order $\xi^{-(1+\alpha)/2}$, so the Harris criterion accordingly gives $\nu \geqslant 2/(1+\alpha)$. Thus, the clean TFIM is perturbatively unstable to weakly hyperuniform potentials, while strongly hyperuniform potentials are marginal. To see that strongly hyperuniform potentials are in fact *irrelevant*, we turn to the exact solution for the zero mode of the TFIM, which can be computed for arbitrary potentials.

### B. Zero mode

As a complementary way of probing the nature of the hyperuniform critical points, we use the following explicit construction of the zero mode of the critical Ising Hamiltonian [25]:

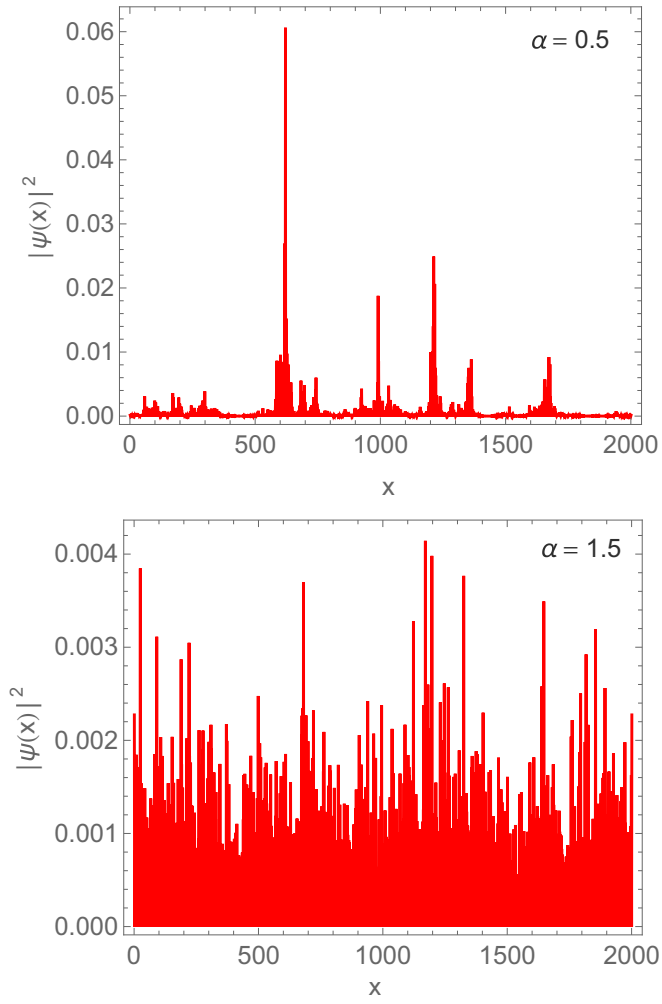


FIG. 4. Zero-mode wave-function profiles $|c_i|$ [see Eq. (5)] in a representative sample in the weakly (left) and strongly (right) hyperuniform regimes.

$$\eta_0 = \sum_i c_i \gamma_i, \quad c_i = \frac{1}{\mathcal{N}} \prod_{j<i} (h_j/J_j), \tag{5}$$

where $\mathcal{N}$ is a normalization factor. Since strongly hyperuniform potentials do not cause this product to wander, the zero mode has uncorrelated random site-to-site fluctuations but no large-scale heterogeneity. For instance, in the $\alpha = 2$ model, $J_i = J \exp(s\{\xi_i - \xi_{i-1} + 1\})$, $h_i = h \exp(s)$ so $c_i \propto (h/J)^i \exp(-\xi_i - \xi_1) \sim \exp(-\xi_i)$ at criticality. In the weakly hyperuniform case, by contrast, $\eta_0$ has strong amplitude fluctuations (Fig. 4), with sharp isolated peaks $c_j$. Moving a distance $l$ away from a peak, at criticality, the wave-function amplitude typically decays as $c_{j+r} \sim \exp(-\text{const} \times |r|^{(1-\alpha)/2})$. In the marginal case $\alpha = 1$, the product decays as $c_{j+r} \sim \exp(-\text{const} \times \sqrt{\ln r})$ away from the peak $c_j$, i.e., slower than any power law. Therefore, we expect the zero mode in this case to be spread out uniformly over the lattice, as in the strongly hyperuniform regime.

### C. Energy-dependent localization length

In the models we are considering here, states far from $E = 0$ are localized, with a localization length $\xi$ given (at weak disorder) by the theory of weak localization

$$\frac{1}{\xi(E_k)} \sim \rho(E_k)([J_k J_{-k}] + [h_k h_{-k}]) \sim \rho(E_k) S_\alpha(k, k), \quad (6)$$

where $E_k$ is the clean dispersion, and $J_k, h_k$ are the appropriate Fourier components of the hyperuniform potential. To obtain this result, consider a plane wave of momentum $k$, and treat the disorder perturbatively. The mean-free distance is calculated by taking the product of the Fermi's golden rule decay time of the plane wave, and the group velocity. As the mean-free distance is the only length scale in the problem, we identify it with the localization length, yielding Eq. (6).

A consequence of Eq. (6) is that the behavior of the localization length as $|E| \to 0$ is sensitive to $\alpha$. Specifically, if we begin at the clean critical point, and consider the weak-localization formula for $\xi$ as $|E| \to 0$, we find that $\xi \sim 1/|E|^\alpha$. This perturbative result is internally consistent whenever $k\,\xi(E_k) \gg 1$, where $k \propto E$ at the critical point; this is true for weak disorder when $\alpha \geqslant 1$, but breaks down as $|E| \to 0$ when $\alpha < 1$. Physically, in the strongly hyperuniform regime, the localization length diverges sufficiently rapidly at low energies that the momentum of an eigenstate $\sim|E|$ becomes asymptotically sharp compared to its momentum width $|E|^\alpha$, although the wave function is localized on the longest scales. By contrast, in the weakly hyperuniform regime, as with uncorrelated disorder, the perturbation theory breaks down at sufficiently low energies, and the low-energy localization properties are governed by nonperturbative effects.

### D. Stability of the critical Ising insulator

The strongly hyperuniform case shares some features with the putative semimetal-to-metal critical point in disordered Weyl and Dirac systems [54–57]. For Weyl systems, it is the zero-energy density of states (DOS) rather than the spectrum of the disorder that vanishes at low energies; however, both mechanisms cause disorder to be perturbatively irrelevant as $|E| \to 0$. Nonperturbative rare-region effects destabilize Weyl semimetals in the presence of disorder, and one might wonder if some similar nonperturbative effect might arise as $|E| \to 0$ at the strongly hyperuniform critical point, leading it to flow to strong randomness. If some such scenario held, we would expect the true critical point to be at infinite randomness regardless of $\alpha$, and the structure of the zero mode to evolve smoothly with $\alpha$. But, as we saw above, the exact zero mode in fact shows an abrupt change of behavior at the critical value $\alpha = 1$, supporting our case that there really is a sharp change in the critical properties between weakly and strongly hyperuniform regimes.

## IV. STRONGLY HYPERUNIFORM CASE: "CRITICAL ISING INSULATOR"

In this section we explore the critical behavior of the thermodynamics, equal-time correlations, transport, and dynamics when $\alpha > 1$. As noted already, the critical point has

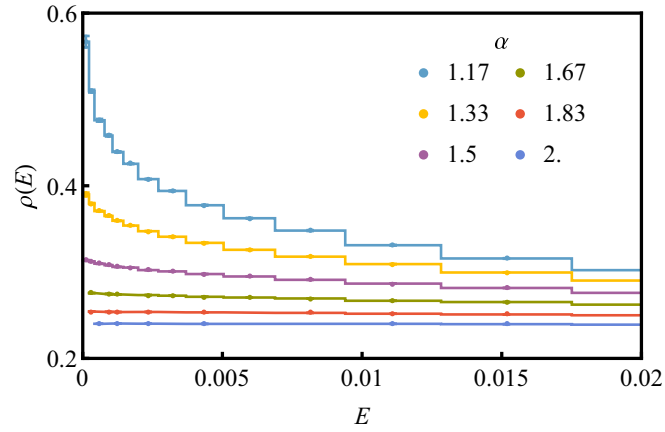


FIG. 5. Density of states for strongly hyperuniform systems. At low energies the density of states tends to a finite value as in the clean case. The hyperuniform modulation gives rise to a subleading correction in the form of a nonanalytic cusp. The density of states was computed using the recursive method of Ref. [58] for parameters $L = 10^7$, $s = \frac{3}{16}$, and $n = 40$ disorder realizations.

an energy-dependent localization length

$$\xi(E) \sim 1/|E|^\alpha; \quad (7)$$

this relation will be central to our analysis below. We first summarize the equilibrium properties of the critical point, which are (to leading order) unchanged by the hyperuniform potential; then turn to its dynamical properties, which are qualitatively different from those of the clean system. Finally, we extend our results away from the critical point.

### A. Equilibrium properties

#### *1. Density of states*

Since disorder is perturbatively irrelevant at this critical point, we expect the DOS of the disordered problem to approach a constant as $E \to 0$. However, there is a subleading nonanalyticity in the DOS, for $\alpha \neq 2$. This nonanalyticity follows from the nonanalytic behavior of $\xi$; in fact, the two are related by the Thouless formula [59]

$$\int dE'[\rho(E') - \rho_0(E')] \log|E - E'| \simeq \frac{1}{\xi(E)} \sim |E|^\alpha, \quad (8)$$

where $\rho_0(E)$ is the DOS of the clean system. In general, this equality requires $\rho(E) - \rho_0(E) \sim |E|^{\alpha-1}$: thus, the nonanalytic dependence of $\xi^{-1}$ at low energies translates into a nonanalyticity in the DOS. [The case $\alpha = 2$ is special: here, $\xi^{-1}(E)$ is an analytic function of $E$, so the nonanalytic DOS correction is absent there.] We see this nonanalytic behavior clearly by numerically evaluating the DOS for very large systems via the recursion method of Ref. [58] (Fig. 5). Finally, we note that due to the subleading nature of the correction to DOS we have neglected to precisely calculate logarithmic corrections in (8).

#### *2. Equilibrium correlation functions*

On dimensional grounds, we expect equilibrium correlation functions at long distances to behave as they would

for clean systems. The scale $\xi_l \sim 1/|E|^\alpha$ is much larger than $\ell_{\text{Ising}} \sim 1/E$. In the clean system, the correlations at a length scale $l$ are set by wave functions at energies $E \sim 1/l$; however, these wave functions are only localized on much longer scales, so their localization properties are irrelevant for the equilibrium correlations. This expectation is consistent with the results of numerical simulations (Sec. VI).

### B. Dynamics at the critical point

#### 1. Thermal transport

Unlike equilibrium properties, transport is strongly modified by localization. The simplest conserved quantity in the Ising model is energy; accordingly, we focus on thermal transport. In the clean Ising chain, thermal transport is ballistic and the conductance is given by the appropriate Landauer formula $\kappa \sim T$ [60]. This result no longer applies in the CII, but understanding how precisely energy is transported requires some care with the order of limits. In what follows, we consider a setup in which the Ising chain is connected to two leads at temperatures $T_{\text{L}} \equiv T - \Delta T/2$ and $T_{\text{R}} \equiv T + \Delta T/2$, respectively; we also make the linear-response assumption $\Delta T \ll T$.

Since $\xi \sim 1/|E|^\alpha$, in a chain of length $L$, excitations with $E \lesssim 1/L^{1/\alpha}$ are delocalized (and indeed ballistic). Since the level spacing scales as $1/L$, the *number* of delocalized modes grows with system size, although the delocalized fraction of the spectrum decreases as $L^{-1/\alpha}$. There is a mesoscopic parameter regime for the temperature gradient such that $1/L \ll \Delta T \ll T \ll 1/L^{1/\alpha}$. In this mesoscopic regime, heat transport takes place through the delocalized states around zero energy and the clean-system Landauer result [60] continues to apply.

However, for thermodynamically long chains, this is not the appropriate order of limits. Instead, one keeps $\Delta T$ finite as $L \to \infty$, so that $1/L^\alpha \ll \Delta T \ll T$. In this limit, a vanishing fraction of the modes around $E = 0$ contribute to transport; moreover, the contribution of each delocalized mode is suppressed because it is effectively at very high temperature. The Landauer formula for the energy flux is [60]

$$\dot{Q} = \frac{1}{2\pi} \int_0^\infty d\omega\, \omega (n_{\text{R}}(\omega) - n_{\text{L}}(\omega)) t(\omega), \tag{9}$$

where $n_{\text{R}}, n_{\text{L}}$ are the quasiparticle occupation numbers in the two leads, and $t(\omega)$ is the transmission coefficient of states at frequency $\omega$. The transmission coefficient is given by $\exp(-L/\xi) \sim \exp(-\alpha L E^\alpha)$, which we approximate by cutting off the integral at the energy scale $1/L^{1/\alpha}$ (this amounts to neglecting the exponentially suppressed transmission through localized states). The delocalized states with energies $E \lesssim 1/L^{1/\alpha}$ have occupation numbers that are effectively at high temperature since $1/L^{1/\alpha} \ll T$. Thus, $n_{\text{R}}(\omega) \sim 1/2 - \omega/T_{\text{R}}$, and likewise for $n_{\text{L}}$. Plugging these results into (9) we find

$$\dot{Q} \sim \frac{\Delta T}{T^2} \frac{1}{L^{3/\alpha}} \Rightarrow \kappa \sim \frac{1}{T^2 L^{3/\alpha}}, \tag{10}$$

so the critical state is a thermal insulator, with a conductance that decays algebraically with chain length.

TABLE I. Scaling properties of $\{\gamma_{i+r}(t)\gamma_i(0)\}$ in the strongly hyperuniform regime ($1 < \alpha \leqslant 2$).

| Quantity | Behavior |
|---|---|
| Front height | $t^{-2/\alpha} \sim r^{-2/\alpha}$ |
| Front width | $t^{1/\alpha} \sim r^{1/\alpha}$ |
| Late-time saturation value | $r^{-1-1/\alpha}$ |

#### 2. Wave-packet dynamics and autocorrelations

We now turn to the behavior of autocorrelation functions and wave-packet dynamics; these quantities might be easier to probe, e.g., in ultracold atomic experiments, than transport. A particularly illuminating quantity to study is the dynamics of the Majorana fermion operator describing to the spreading of elementary excitations

$$\gamma_i(t) = e^{iHt} \gamma_i e^{-iHt} = \sum_j U_{ij}(t) \gamma_j, \tag{11}$$

the transition matrix is set by the anticommutator $U_{ij}(t) = \{\gamma_i(t), \gamma_j(0)\}$. This quantity is closely related to the out-of-time-order correlator [61,62]. After addressing how elementary excitations spread, we turn to the behavior of general autocorrelation functions.

In the clean system at its critical point, operators spread ballistically. The situation in the disordered case is quite different. One can decompose the spatial Majorana degrees of freedom in terms of the fermionic eigenmodes $\gamma_i = \sum_n u_{in} \eta_n$. After time evolution up to a timescale $t$, the projection of $\gamma_i$ onto modes that have localization lengths $\xi \lesssim t$ remains localized, while the rest of the operator moves ballistically to the light cone $r(t) = t$. Assuming the operator was initially spread out uniformly among modes, the fraction that is still spreading at time $t$ is $1/t^{1/\alpha}$. This spreading fraction consists of a well-defined but broadening peak, which is Gaussian in its outer tail, with height decaying as $t^{-2/\alpha}$ and width broadening as $t^{1/\alpha}$. As it moves, the front locally "deposits" intensity of order $t^{-1-1/\alpha}$ (one can see this from the conservation of total weight). When $\alpha > 1$ (i.e., in the CII), the height of the "deposited" operator is parametrically smaller than the height of the front, and the front remains well defined at late times (Fig. 6).

Finally, the broadening of the front can be understood as follows. As we noted in Sec. IV A, the DOS in the presence of hyperuniform potentials gets modified to $\rho(E) \sim c + |E|^{\alpha-1}$. Since the momentum of low-energy modes is asymptotically well defined (because the localization length of a mode grows much faster than its wavelength), we can continue to associate a momentum to each eigenstate, and therefore interpret the DOS shift as providing an effective dispersion relation of the form $E(k) \sim a|k| + b|k|^\alpha$. This causes wave packets to spread, with a width $\delta r(t) \sim t^{1/\alpha}$, when $1 < \alpha \leqslant 2$; this is the behavior we observe numerically.[1] These various scaling relations are summarized in Table I. For all $\alpha$ this broadening

[1]For $\alpha > 2$, the leading correction to the dispersion is the (analytic) quadratic term, therefore in this regime the wave packet broadens diffusively, and the height of the front decreases as $t^{-1/\alpha-1/2}$.

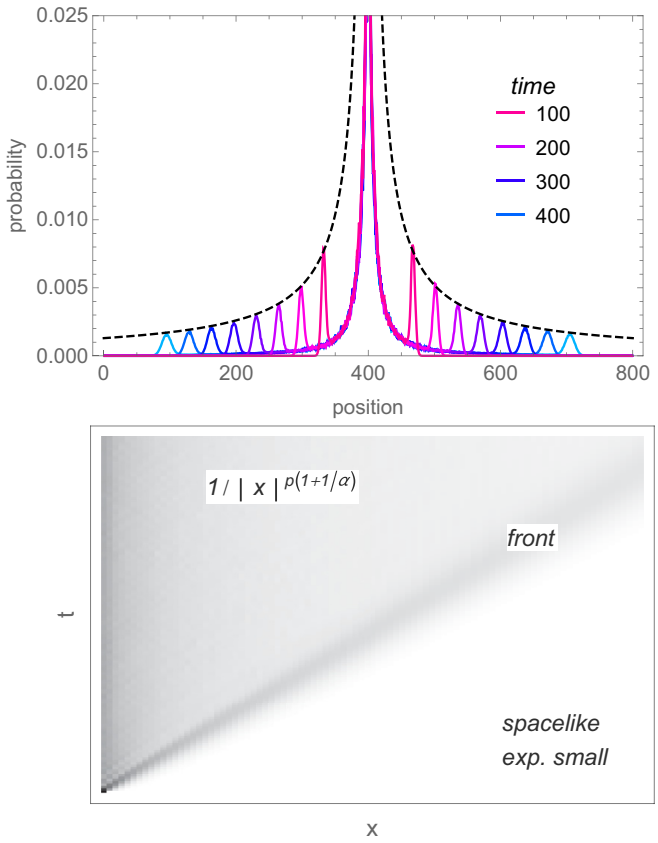


FIG. 6. Top: spreading of a wave packet at the critical point for $\alpha = 2$. A well-defined ballistic front exists and moves out with the clean critical velocity; however, the weight at the front attenuates with time: its height shrinks as $1/t$ (dashed line) and it broadens as $\sqrt{t}$ (Supplemental Material, Appendix A [73]). Bottom: regimes of $\{\gamma_{i+r}(t), \gamma_i(0)\}$. The autocorrelator is small outside the light cone, grows to $r^{-2/\alpha}$ when $r \sim t$, then saturates at later times to a value $\{\gamma_{i+r}(\infty), \gamma_i(0)\} = 1/r^{1+1/\alpha}$. Other correlation functions can exhibit multiples $p = 1, 2, \ldots$ of this basic power law.

parametrically exceeds the $t^{1/3}$ broadening in the clean Ising chain [63–67].

Because the TFIM is a model of free fermions, the results above can be used to infer the dynamics of any local perturbation that preserves the Ising symmetry (i.e., does not involve Jordan-Wigner strings). The various regimes of behavior of spatiotemporal autocorrelation functions such as, e.g., the retarded transverse-field autocorrelation function $\langle[\gamma_i(t)\gamma_j(t), \gamma_0(0)\gamma_1(0)]\rangle\Theta(t)$, can also be deduced from the structure of the Heisenberg operator $\gamma_i(t)$. In the TFIM, local operators locally create or eliminate some number of quasiparticles, and each of these quasiparticles behaves as discussed above. Space-time correlation functions exhibit a well-defined but rapidly attenuating light cone, and the behavior inside the light cone clearly indicates localization: the memory of local perturbations persists indefinitely. The regimes of behavior of local autocorrelation functions are sketched in Fig. 6. If one fixes a distance $r$ and measures a generic correlation function $C(r, t)$, it has three regimes: (i) at times before the light cone passes through, the correlation function is small, as causality demands; (ii) at a time $r \sim t$, the correlation function grows to a value that is power-law small in $r$; (iii) at times $r \gg t$, it saturates to a parametrically smaller value that is also power-law small in $r$. The precise values of these exponents depend on the operator.

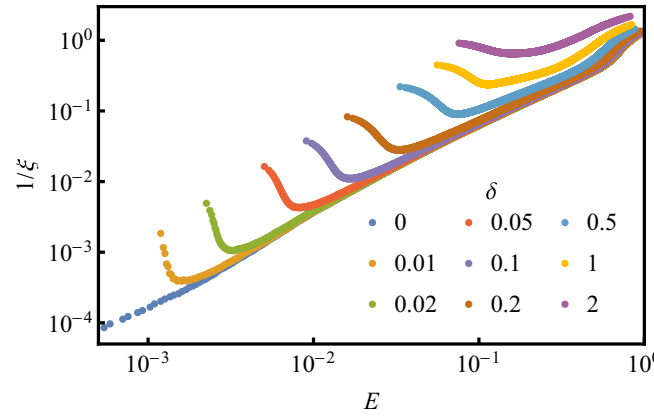


FIG. 7. Minimum in the inverse localization length $1/\xi(E)$: disorder averaged $1/\xi$ is plotted versus $E$. At criticality the localization length $\xi$ is monotonically increasing with decreasing excitation energy $E$. When one detunes away from criticality by $\delta$, the localization length is minimized at an energy $E = O(\delta)$. Data for system sizes $L = 5000$, $\alpha = 1.5$, $s = \frac{3}{16}$ error bars smaller than plot points.

### C. Away from criticality

#### *1. Localization length*

Away from criticality, it appears that all states are localized at weak disorder. For simplicity, we consider the paramagnetic phase (though our results extend to the ferromagnetic phase by Ising duality). Here, the clean system is gapped, with a dispersion relation $E \sim \sqrt{\Delta^2 + k^2}$. We are primarily concerned with the localization properties near $k = 0$, which correspond to $E = \Delta$. The density of states is $\rho(E) \sim 1/\sqrt{E - \Delta}$, and the effective velocity of an excitation at $k(E) \sim \sqrt{(E - \Delta)\Delta}$ is $v(E) \sim \sqrt{E - \Delta}$. At leading order in perturbation theory, we find that the mean-free *time* diverges in the strongly hyperuniform regime as $\tau(E) \sim (E - \Delta)^{1/2(1-\alpha)}$. However, because the velocity vanishes as $E \to \Delta$, the mean-free path goes as $\xi(E) \sim (E - \Delta)^{1-\alpha/2}$. Thus, $\xi$ vanishes (and perturbation theory ceases to be controlled) near the bottom of the band for $1 \leqslant \alpha < 2$. We check numerically that $\xi$ does indeed decrease near the bottom of the band in Fig. 7. Precisely, the pairs $\psi^n, E_n$ were obtained by exact diagonalization of a periodic chain, and indexed $n$ by their rank order in energy. A localization length $\xi_n$ is then assigned to each one by a least-squares fit to the relationship

$$\log \sum_i \left|\psi_i^n \psi_{i+r}^n\right| = r/\xi_n + \text{const} \tag{12}$$

for $-L/2 < r < L/2$. The ensemble averaged values of $1/\xi = [1/\xi_n]$ and $E = [E_n]$ are then plotted in Fig. 7.

For $\alpha = 2$, the localization length remains finite at the bottom of the band, and for $\alpha > 2$ it diverges within perturbation theory. Even for $\alpha > 2$, however, rare local configurations of the potential might smooth out the square-root divergence

of the DOS and thus prevent $\xi$ from diverging; this issue is outside the scope of this work.

#### 2. Equilibrium correlations

The equilibrium correlation length at a distance $\delta$ from criticality is governed by the slowest-decaying modes in the system. The very lowest-energy modes are potentially tightly localized, in which case they cannot transmit correlations beyond their localization length; however, modes at an energy $\Delta E \sim \delta$ from the bottom of the band are still "critical" regime, so their localization lengths are parametrically larger than their inverse momenta, provided $\delta$ is sufficiently small. Thus, the correlation length of the system is governed by these modes, which decay on a length scale set by the distance from criticality, *not* the localization length. Thus, up to potential numerical factors, the equilibrium behavior of the model away from criticality should be identical to that of the clean system. The minima in $1/\xi(E)$ which govern this behavior are visible in Fig. 7.

#### 3. Transport and dynamics

Unlike equilibrium correlations, transport and dynamics are strongly affected by the localization properties of the model. For $\alpha \leqslant 2$ all modes are localized, with a nondiverging $\xi$. Wave packets do not travel to infinity, and the finite-temperature thermal transport coefficients are *exponentially* small in system size (in addition to being thermally activated). Specifically, at a distance $\delta$ from criticality, the least localized modes are those with $\Delta E \sim \delta$ above the gap, which have localization length $\xi \sim 1/\delta^{\alpha}$ (see Fig. 7). The conductance through a system of length $L$ is therefore suppressed as $\exp(-L\delta^{\alpha})$.

## V. WEAKLY HYPERUNIFORM CASE: INFINITE-RANDOMNESS CRITICAL LINE

While perturbation theory about the clean limit allowed us to extract the behavior of physical observables in the strongly hyperuniform case (even when this behavior was drastically different from the clean system), such a perturbative approach evidently fails when disorder is relevant at the critical point. We approach this regime instead using strong-disorder renormalization-group (SDRG) methods and estimates based on counting rare regions. We first discuss the behavior of the density of states at the critical points, and the absence of Griffiths phases for $\alpha > 0$, as these can be understood using elementary counting arguments. We then present SDRG results for the evolution of critical exponents with $\alpha$. This section focuses on static properties, as these are the most directly accessible; however, we expect the dynamics throughout this phase to be qualitatively similar to that at the conventional infinite-randomness critical point.

### A. Density of states

The thermodynamic properties of the critical point are captured by the density of states (DOS) near zero energy; this quantity can be estimated by adapting Ref. [68]. The key result of that work is that, for a random hopping model, the integrated DOS up to energy $E$, $N(E) = \int_0^E \rho(E')dE'$, obeys the relation $N(E) \sim 1/2\ell(E)$, where $\ell$ is the spatial scale over which the quantity $\log[\prod_j J_j/h_j]$ changes by an amount $\sim \log E$. For uncorrelated randomness, $\ell \sim \log^2 E$, leading to the familiar Dyson singularity in the DOS. For strongly hyperuniform potentials, when the potential is weak enough, the wandering does not grow with distance at all, so $\ell = \infty$, and the DOS is (to leading order) unaffected by weak randomness (but as discussed in Sec. IV, there are subleading nonanalyticities). For $\alpha < 1$, $\ell \sim \log^{2/(1-\alpha)}(E)$ and therefore $\rho(E) \sim 1/(E \log^{1+2/(1-\alpha)} E)$. The corresponding low-energy behavior of the integrated DOS for weakly hyperuniform disorder, $N(E)^{(\alpha-1)/2} = c_1 \log E + c_0$ (for some constants $c_0, c_1$), is verified in Fig. 8. This construction of the DOS also gives an implicit relation between length scales and timescales, $\ell(E)$. In the strongly hyperuniform case, $\ell(E) = \infty$, so randomness does not affect the dynamic critical exponent. In the weakly hyperuniform case, $\ell(E) \sim \log^{2/(1-\alpha)}(E)$, suggesting infinite-randomness behavior. For $\alpha = 1$, $\sqrt{\log \ell} \sim \log E$, so $\ell \sim \exp(\text{const} \times \log^2 E)$. Thus, $\rho(E) \sim e^{-\text{const} \times \log^2 E} \log E/E$, which vanishes at small $E$. This is subleading to the perturbative effects discussed in the previous section (as we would expect since $\alpha = 1$ is in effect strongly hyperuniform).

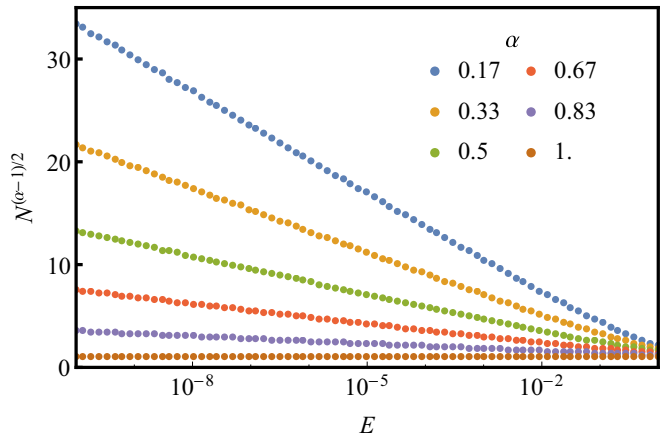


FIG. 8. Density of states for weakly hyperuniform systems. At low energies the integrated density of states scales as $N(E)^{(\alpha-1)/2} = c_1 \log E + c_0$ (for constants $c_0, c_1$), generalizing the familiar $N(E) \sim 1/\log^2 E$ of the iid ($\alpha = 0$) case. Mean values of $N(E)$ are calculated by disorder averaging; statistical error is shown by error bars. Parameters: $L = 10^7$, $s = \frac{3}{16}$.

### B. Griffiths effects

The infinite-randomness critical point at $\alpha = 0$ is associated with "Griffiths" regimes on either side; in these regimes, the response to perturbations is dominated by rare regions that are in the wrong phase, and these contributions are parametrically dominant over the response from typical regions. Thus, for instance, in the paramagnetic phase sufficiently near the transition, the magnetization $m(h) \sim h^{\gamma}$ with $\gamma < 1$. This behavior occurs because the paramagnet contains an exponentially small (in size) density of regions that are locally in the ferromagnetic phase, and these regions have an exponentially large contribution to the susceptibility. These two

exponentials combine to give a continuously varying power law, depending on the density of Griffiths regions, and the power law is less than one close to the critical point.

For $\alpha > 0$, there are no Griffiths regimes. One can see this by estimating the number of rare ferromagnetic regions in the microscopic model (i.e., regions of size $l$ for which the local control parameter $\delta_l$ exceeds some threshold $\beta$). To do this, we need the probability distribution $P_L(\delta_l)$ for a region of size $l$. It is simpler to work with the characteristic function

$$F_l(t) \equiv \left[ \exp\left( \frac{it}{l} \sum_{j=1}^{l} \ln\left\{ \frac{h_j}{J_j} \right\} \right) \right] \sim \exp(-t^2 l^{-(\alpha+1)}), \tag{13}$$

where we used the Gaussian (though correlated) nature of the distribution of $\ln(h_i/J_i)$. Inverting the Fourier transform, we find

$$P_l(\delta_l) \sim \exp\left( -\delta_l^2 l^{1+\alpha} \right). \tag{14}$$

Thus, the probability of a ferromagnetic region is suppressed faster than exponentially in $l$, whenever $\alpha > 0$. (In the strongly hyperuniform regime, it vanishes as a Gaussian in $l$, which is natural since in this regime the entire variance must come from the edge spins, which have a Gaussian distribution.)

We now estimate the contribution to the susceptibility from these regions. At a field $h$, the ferromagnetic regions of size $\gtrsim \log h$ fully magnetize. The density of such regions is given by $\exp[-(\log h)^{1+\alpha}]$. This vanishes faster than a power law at small $h$, so it is always subleading to the paramagnetic response from typical regions.

The arguments above applied only to the bare couplings; one might wonder if they continue to apply if one instead considers renormalized couplings. We argue below (Sec. V C), after introducing our renormalization scheme, that they do apply.

#### *Edge-spin susceptibility*

This analytic argument against Griffiths effects is borne out numerically by studying the magnetization of the chain in response to a field applied at the edge; this is a simple way of computing a lower bound to the susceptibility of Ising chains (Fig. 9). To do this within the free-fermion description of the TFIM, one can introduce an artificial edge spin $\tau_0$ at one end of the chain, which couples to the leftmost spin via a coupling $g\tau_0^x\tau_1^x$ but has no transverse field acting on it [69]. The susceptibility of the edge spin to this field is given by the $g$ dependence of the quantity $\langle \tau_0^x \tau_1^x \rangle$, which we can compute within the free-fermion theory. Our results are consistent with the absence of a Griffiths phase at $\alpha > 0$: the low-field susceptibility appears to be asymptotically linear in the field even very close to the critical point, in contrast to the $\alpha = 0$ case.

### C. SDRG and correlation functions

To probe the nature of the critical point in the weakly hyperuniform case, we numerically apply the standard SDRG for the random TFIM [8–10,70,71] to the hyperuniform case.

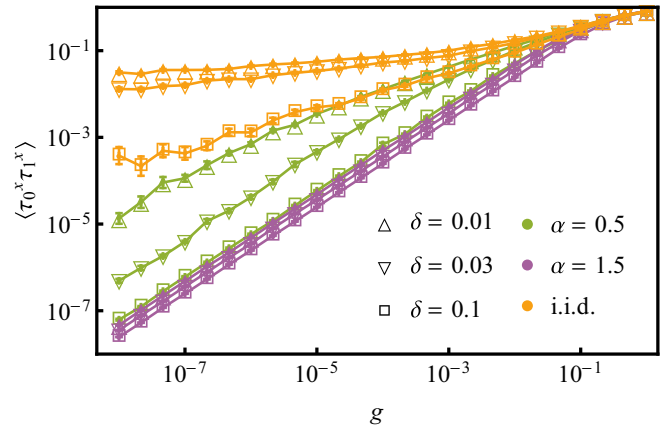


FIG. 9. Susceptibility of a spin at the edge of the chain vs distance from the transition $\delta$, for the cases $\alpha = 0$ (independent random couplings), $\alpha = 0.5$ (weakly hyperuniform), and $\alpha = 1.5$ (strongly hyperuniform). Evidently, even for weakly hyperuniform couplings, the susceptibility approaches linear behavior with field even very close to the transition, suggesting the absence of a Griffiths phase. Parameters: $L = 2000$, $s = \frac{3}{16}$.

The SDRG rules involve picking the largest coupling and eliminating it. If the largest coupling is a bond, one creates a new effective spin with transverse field $h_i h_{i+1}/J_i$; if the largest coupling is a field, one eliminates the corresponding spin to create a new effective bond $J_i J_{i+1}/h_i$. An important property of these rules is that the effective bonds at any stage in the SDRG are products of microscopic $J_i$ divided by products of microscopic $h_i$, and vice versa for the fields. If one runs the RG until the system size is rescaled by a factor $l$, the typical coupling scales as $\prod_{j=i}^{i+l}(J_j/h_j) \sim \exp(-\text{const} \times l^{(1-\alpha)/2})$. Thus, the space-time scaling at this critical point has the infinite-randomness form $t \sim \exp(\text{const} \times l^{\psi})$, with $\psi = (1-\alpha)/2$.

Other key exponents, such as the scaling of mean cluster moments, can be extracted from numerically iterating the SDRG rules for large systems (Fig. 10). The mean cluster moment $\mu$ at a length scale $\ell$ goes as $\mu \sim l^{\psi\phi}$, where $\psi\phi$ decreases linearly from its $\alpha = 0$ value as $\alpha$ is increased. Thus, hyperuniformity yields sparser spin clusters than iid randomness. In the uncorrelated case, the mean cluster moment and the exponent that governs decay of mean order-parameter correlations are related: $C_{xx}(r) \sim 1/|r|^{2\Delta_\sigma}$, where $\Delta_\sigma = 1 - \psi\phi$. We find numerically that this relation continues to hold for the weakly hyperuniform case (as one might expect, since the argument for this relation in Ref. [9] is quite general).

A surprising implication of our results is that mean correlations at the critical point actually decay *faster* in the weakly hyperuniform case than in the uncorrelated case (although the decay in the uncorrelated case is already faster than in the clean TFIM). Thus, as one tunes $\alpha$, it seems the exponent $\Delta_\sigma$ must first increase, and then discontinuously decrease to the clean Ising value at $\alpha = 1$. By contrast, the *typical* correlations keep getting longer ranged as the degree of hyperuniformity increases, going as $\exp(-|r|^{\psi})$. These observations can be qualitatively reconciled as follows: Hyperuniformity

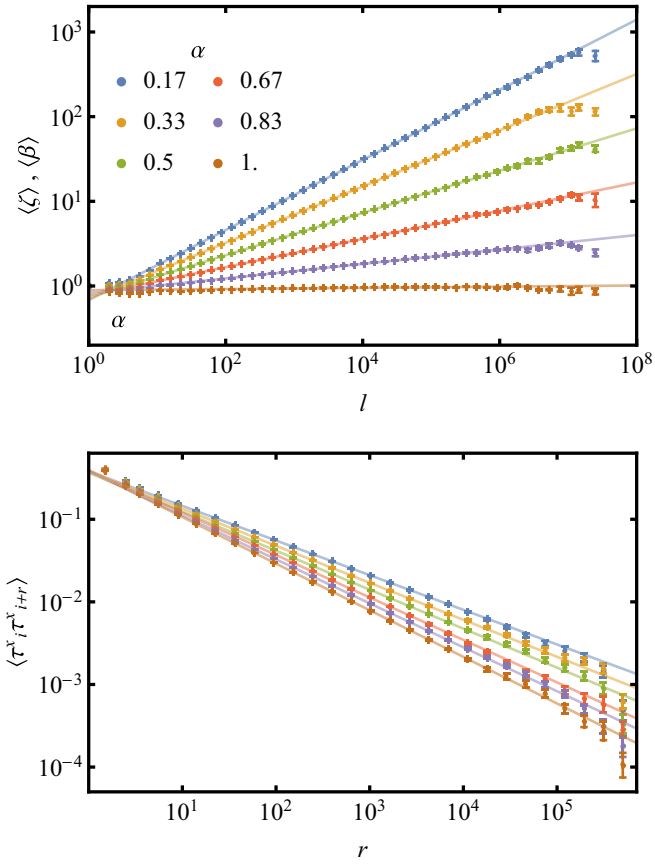


FIG. 10. Strong-disorder RG exponents. Upper panel: flow of typical coupling scale $[\zeta], [\beta]$ vs length scale $l$ under SDRG for various values of $\alpha$. The power law $[\zeta], [\beta] \sim l^{\psi}$ is exhibited with exponent $\psi = (1-\alpha)/2$. Lower panel: average correlator $C_{xx}(r) = \langle\tau^x_i\tau^x_{i+r}\rangle$ as a function of spacing. The decay is algebraic, and fits to the form $C_{xx}(r) \sim 1/r^{2(1-\psi\phi)}$ where the typical moment at scale $l$ scales as $\mu \sim l^{\psi\phi}$ (scaling of moments is shown in the Supplemental Material, Appendix C [73]). Parameters: $L = 10^8$, $s = \frac{3}{16}$.

involves local anticorrelations, which make spin clusters sparser than for independent randomness; therefore, correlations due to rare clusters are suppressed. At the same time, $\psi$ decreases so typical correlations become longer ranged. Eventually, at $\alpha = 1$, typical regions begin to dominate over rare regions, and one enters the strongly hyperuniform regime.

### *Griffiths effects*

We now return to the question of whether Griffiths phases exist. This was already addressed for the bare theory in Sec. V B; we now argue that renormalization does not change this basic conclusion. Consider running the RG out to some finite length scale $\ell$; at this scale, the system consists of effective spins consisting of $O(\ell)$ microscopic spins, subject to transverse fields of the form $\tilde{h} = (h_k h_{k+1} h_{k+2} \ldots h_{k+\ell})/(J_{k+1} J_{k+2} \ldots J_{k+\ell})$, and coupled by bonds $\tilde{J}$ that are likewise products of adjacent $J$'s divided by products of adjacent $h$'s. Suppose we take a region of size $l \gg \ell$. The wandering in this region obeys the identity $\tilde{\delta} = \sum_\alpha \log(\tilde{J}_\alpha/\tilde{h}_\alpha) = \sum_i \log(J_i/h_i) = \delta$, where $\alpha$ labels the $o(l/\ell)$ effective spins and $i$ denotes the original microscopic spins in that region: this identity is an immediate consequence of the SDRG rules. Thus, if one terminates the RG after finitely many steps, the asymptotics of the wandering on much larger scales are unaffected, and the argument of Sec. V B goes through.

## VI. EXACT DIAGONALIZATION RESULTS FOR CORRELATION FUNCTIONS

The previous sections addressed the properties of the weakly and strongly hyperuniform cases, using different methods (perturbation theory and SDRG, respectively). In this section we discuss how correlation functions evolve as one tunes $\alpha$, using exact diagonalization. We first discuss two-point spin correlations, and then the ground-state entanglement entropy.

### A. Spin-spin correlations

The free- fermion character of the Ising model allows us to perform simulations on systems of up to a few thousand sites. We focus on the equal-time correlation function of the order parameter $C_{xx}(r) \equiv \langle\tau^x_i\tau^x_{i+r}\rangle$; this can be expressed as a determinant of free-fermion Green's functions [28]. We have checked that correlation functions evolve qualitatively similarly. We set the disorder strength $s = \frac{3}{16}$: when the disorder is either much weaker or much stronger, we see strong transients. For weak disorder, these transients are expected, as the system is clean on short scales. At strong disorder, the states away from $E = 0$ are effectively site localized and do not see the hyperuniformity; the universal regime of $\xi(E)$ shrinks to very small energies or equivalently to very large length scales.

Our numerical results for the typical and average correlations are plotted in Fig. 11. Both typical and mean correlations behave differently in the two regimes. In the strongly hyperuniform case, we see clean critical behavior in both mean and typical correlations. In the weakly hyperuniform case, typical correlations are consistent with a stretched exponential, with the appropriate exponent $\langle\tau^x_i\tau^x_{i+r}\rangle \sim \exp(-\text{const} \times r^{\psi})$. Mean correlations clearly decay with a steeper power law than the clean theory would suggest; however, at the accessible system sizes we cannot clearly identify a regime of power-law scaling. A clearer sign of the difference between the two regimes can be seen by considering the histogram of $C_{xx}(r)$ in the two cases (Fig. 12). These histograms broaden with $n$ in the weakly hyperuniform case but stay the same width (on a logarithmic scale) in the strongly hyperuniform case, supporting our picture that the weakly hyperuniform case is at infinite randomness.

### B. Ground-state entanglement entropy

The ground-state entanglement entropy provides a useful probe of criticality. In particular, the ground-state entanglement $S_\ell$ between the first $\ell$ sites of an open chain and the remaining sites $(\ell+1, \ldots, L)$ grows as

$$S_\ell = \frac{c}{6}\log\ell + c_1' + O(\ell/L), \tag{15}$$

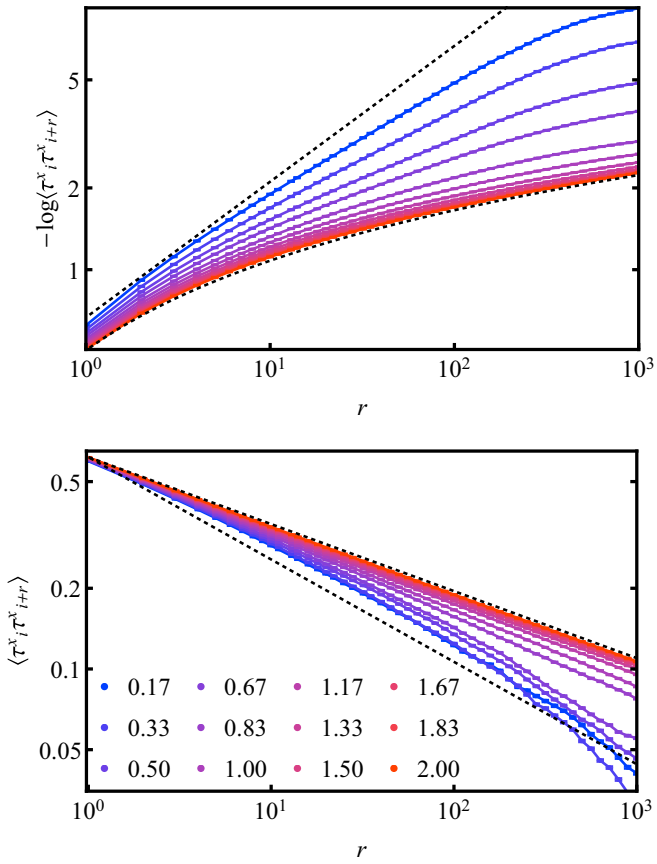


FIG. 11. Typical (upper) and mean (lower) order-parameter correlation functions $\langle\tau^x_i\tau^x_{i+r}\rangle$ as a function of distance for different $\alpha$ (legend inset). The behavior of the typical correlation function is consistent with a power law in the strongly hyperuniform case ($\alpha > 1$) and with a stretched exponential in the weakly hyperuniform case ($0 < \alpha < 1$). The mean correlator decays with the clean Ising exponent in the strongly hyperuniform case, but clearly faster in the weakly hyperuniform case. In the weakly hyperuniform case we do not see a clean power law at large scales; it seems that our data here are still dominated by typical rather than mean behavior. Parameters: $L = 2000$ periodic chain, $s = \frac{3}{16}$.

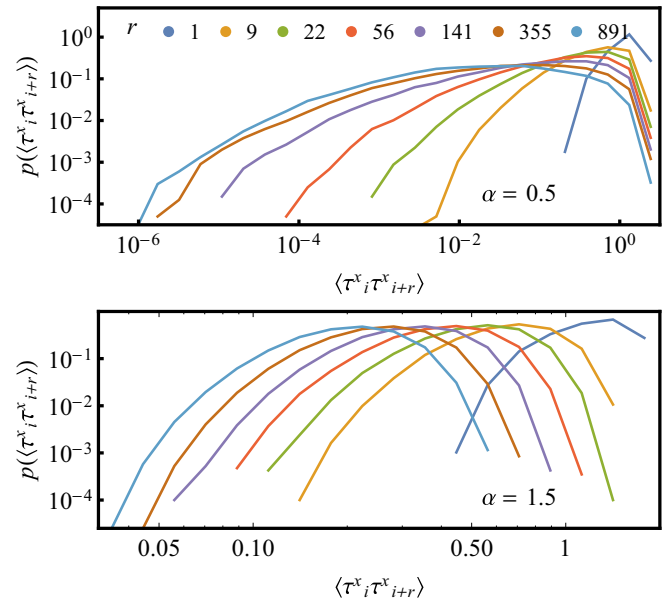


FIG. 12. Histograms of the order-parameter correlation function $\langle\tau^x_i\tau^x_{i+r}\rangle$ for exponentially spaced values of $r$, for weakly hyperuniform (upper) and strongly hyperuniform (lower) systems. In the former case, the histograms broaden strongly, while in the latter case they do not broaden. Parameters: same as Fig. 11.

where the coefficient $c$ forms part of the universal content of the scaling theory, and $c_1'$ is a nonuniversal constant. If the scaling limit is described by a conformal field theory, $c$ is equal to the corresponding central charge. This applies to the clean Ising critical point, where $c = \frac{1}{2}$. In the disordered case there is no underlying conformal field theory, but nonetheless the coefficient $c$ is still fixed by the universal content of the scaling theory. Notably in the case of uncorrelated random disorder, where the transition is described by the infinite-randomness critical point, direct calculation yields $c = \frac{1}{2}\log 2$ [72].

In this section we numerically extract the coefficient $c$ from the logarithmic growth of the entanglement entropy (15). For $\alpha > 1$, we find $c = \frac{1}{2}$, consistent with the clean Ising universality exhibited throughout the strongly hyperuniform regime. In contrast, in the weakly hyperuniform regime, the universality is altered, and we find results which indicate the coefficient $c$ is given by a linear interpolation between the clean Ising value and the uncorrelated infinite-randomness value

$$c = \begin{cases} \frac{1}{2} & \text{for } 1 \leqslant \alpha \leqslant 2, \\ \frac{\alpha}{2} + (1-\alpha)\frac{\log 2}{2} & \text{for } 0 \leqslant \alpha \leqslant 1. \end{cases} \tag{16}$$

In Fig. 13 we plot the numerically extracted form of $S_\ell - (c/6)\log(L/\pi)$ as a function of $\ell/L$. Plotting in this way causes data corresponding to different $L$ to collapse onto a single scaling form providing $c$ has been correctly identified. In Fig. 13 data are shown for various $L$ (values inset in legend) with the two panels corresponding to values of $\alpha$ from the weakly and strongly hyperuniform regimes, respectively. The data collapse, and exhibit good agreement with $(c/6)\log(\ell/L) + c_1'$ (solid black line) where $c$ is set by (16). The dashed black lines exhibit the expected growth $S_\ell$ for the uncorrelated ($\alpha = 0$, $c = \frac{1}{2}\log 2$) and clean Ising ($\alpha = 1$, $c = \frac{1}{2}$) cases for reference [73].

## VII. DISCUSSION

This work studied a canonical low-dimensional quantum critical point, that of the TFIM, in the presence of random hyperuniform couplings. We have found that the system exhibits two distinct classes of behavior, dependent on the exponent $\alpha$ (or equivalently the wandering exponent $\beta$). These distinct classes of behavior are a line of infinite-randomness critical points, with continuously varying exponent $\psi$, and a "mixed" critical point with the equilibrium behavior of the clean Ising model but the dynamics of an insulator. This "critical Ising insulator" regime shows that disorder can localize excitations (and thus qualitatively modifying critical dynamics) even when it has minimal effects on equilibrium properties; this is of some general conceptual interest, given that static and

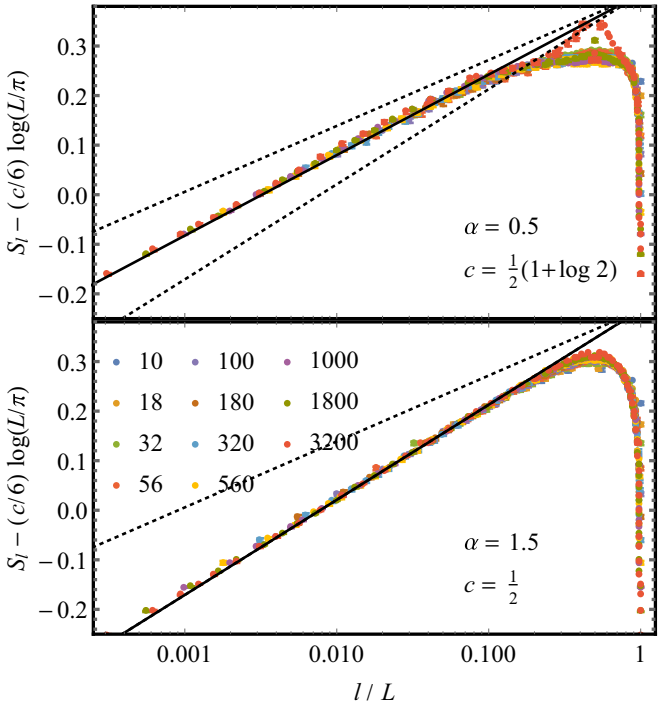


FIG. 13. Entanglement entropy $S_\ell$ of the region $1 \ldots \ell$ as a function of $\ell/L$. The predicted growth is $S_\ell \sim (c/6)\log(\ell)$ (solid black line) with the coefficient $c$ set by (16). The collapse of data for different $L$ (legend inset) onto the predicted line for $\ell \ll L$ validates the conjectured form (16). The dashed black lines exhibit the expected growth of the uncorrelated ($\alpha = 0$) and clean Ising ($\alpha = 1$) cases for reference. The panels correspond to different values of $\alpha$ (values inset), with further data given in the Supplemental Material [73].

dynamical properties are usually intertwined at quantum critical points. Even in the weakly hyperuniform regime, where the strong randomness critical point survives, the Griffiths phases that flank it disappear for hyperuniform couplings, suggesting that hyperuniformity might be a useful knob for controlling Griffiths effects more generally. Using SDRG and perturbation theory, we were able to characterize both critical regimes thoroughly; our predictions are in good agreement with results from exact diagonalization. As is the case with uncorrelated randomness, these results hold for any random modulation with hyperuniform correlations (2), irrespective of other details of the modulation, such as modulation strength or marginal distributions. Generally, these additional properties of the modulation play a role only to determine the length scale above which the asymptotic scaling emerges.

One might wonder how many distinctively hyperuniform critical phenomena exist beyond the TFIM. In general, whenever the control parameter has hyperuniform fluctuations, and there is no source of uncorrelated randomness in the problem, one expects the system will go to a hyperuniform rather than the usual random fixed point. Starting from a microscopic model, however, ensuring that the control parameter fluctuations are precisely hyperuniform on all scales might be challenging. One-dimensional models with multiplicative strong-randomness RG rules are a wide class of models where hyperuniformity holds at all scales. For such models it is crucial that the couplings on odd and even bonds (or $A$ and $B$ sites) remain separately hyperuniform, as in the TFIM. In models such as the TFIM, or spin-1 chains [74], the odd and even bonds are physically different, so it is natural for them to be separately hyperuniform. In the XXZ chain [10], and in toy models of the many-body localization transition [75,76], this is not the case, and this odd-even structure must be imposed by hand if the model is to flow to a hyperuniform fixed point; otherwise, coarse graining disrupts the anticorrelations that cause hyperuniformity (Supplemental Material, Appendix D [73]). Extending these ideas to more general models, as well as to two-dimensional systems [77], is an interesting task for future work.

## ACKNOWLEDGMENTS

We thank V. Alba, A. Chandran, D. Huse, and V. Oganesyan for helpful discussions. The authors acknowledge support from the NSF through Grants No. DMR-1752759 (P.J.D.C.), No. PHY-1752727 (C.R.L.), and No. DMR-1653271 (S.G.). P.J.D.C. acknowledges the financial support of the Sloan Foundation. C.R.L. acknowledges support from the Sloan Foundation through a Sloan Research Fellowship. S.G. performed this work in part at the Aspen Center of Physics, which is supported by NSF Grant No. PHY-1607611. S.G. further acknowledges financial support from a PSC-CUNY internal grant.

[1] A. B. Harris, J. Phys. C: Solid State Phys. **7**, 1671 (1974).
[2] J. T. Chayes, L. Chayes, D. S. Fisher, and T. Spencer, Phys. Rev. Lett. **57**, 2999 (1986).
[3] T. Vojta, Phys. Rev. Lett. **90**, 107202 (2003).
[4] W. De Roeck and F. Huveneers, Phys. Rev. B **95**, 155129 (2017).
[5] J. H. Pixley, D. A. Huse, and S. Das Sarma, Phys. Rev. X **6**, 021042 (2016).
[6] P. A. Lee and T. V. Ramakrishnan, Rev. Mod. Phys. **57**, 287 (1985).
[7] T. Schultz, D. Mattis, and E. Lieb, Rev. Mod. Phys. **36**, 856 (1964).
[8] D. S. Fisher, Phys. Rev. Lett. **69**, 534 (1992).
[9] D. S. Fisher, Phys. Rev. B **51**, 6411 (1995).
[10] D. S. Fisher, Phys. A (Amsterdam) **263**, 222 (1999).
[11] M. Y. Azbel, Phys. Rev. Lett. **43**, 1954 (1979).
[12] S. Aubry and G. André, Ann. Isr. Phys. Soc. **3**, 18 (1980).
[13] J. Biddle, B. Wang, D. J. Priour, Jr., and S. Das Sarma, Phys. Rev. A **80**, 021603(R) (2009).
[14] S. Ganeshan, J. H. Pixley, and S. Das Sarma, Phys. Rev. Lett. **114**, 146601 (2015).
[15] H. P. Lüschen, S. Scherg, T. Kohlert, M. Schreiber, P. Bordia, X. Li, S. Das Sarma, and I. Bloch, Phys. Rev. Lett. **120**, 160404 (2018).

[16] S. Gopalakrishnan, Phys. Rev. B **96**, 054202 (2017).
[17] J. H. Pixley, J. H. Wilson, D. A. Huse, and S. Gopalakrishnan, Phys. Rev. Lett. **120**, 207604 (2018).
[18] M. Schreiber, S. S. Hodgman, P. Bordia, H. P. Lüschen, M. H. Fischer, R. Vosk, E. Altman, U. Schneider, and I. Bloch, Science **349**, 842 (2015).
[19] S. Iyer, V. Oganesyan, G. Refael, and D. A. Huse, Phys. Rev. B **87**, 134202 (2013).
[20] V. Khemani, D. N. Sheng, and D. A. Huse, Phys. Rev. Lett. **119**, 075702 (2017).
[21] Y. B. Lev, D. M. Kennes, C. Klöckner, D. R. Reichman, and C. Karrasch, Europhys. Lett. **119**, 37003 (2017).
[22] M. Žnidarič and M. Ljubotina, Proc. Natl. Acad. Sci. USA **115**, 4595 (2018).
[23] S. A. Weidinger, S. Gopalakrishnan, and M. Knap, Phys. Rev. B **98**, 224205 (2018).
[24] F. Iglói, J. Phys. A: Math. Gen. **21**, L911 (1988).
[25] A. Chandran and C. R. Laumann, Phys. Rev. X **7**, 031061 (2017).
[26] P. J. D. Crowley, A. Chandran, and C. R. Laumann, Phys. Rev. Lett. **120**, 175702 (2018).
[27] P. J. D. Crowley, A. Chandran, and C. R. Laumann, arXiv:1812.01660.
[28] S. Sachdev, *Quantum Phase Transitions* (Cambridge University Press, Cambridge, 2011).
[29] S. Torquato and F. H. Stillinger, Phys. Rev. E **68**, 041113 (2003).
[30] S. Torquato, Phys. Rev. E **94**, 022122 (2016).
[31] Z. Ma and S. Torquato, J. Appl. Phys. **121**, 244904 (2017).
[32] S. Torquato, Phys. Rep. **745**, 1 (2018).
[33] M. Florescu, S. Torquato, and P. J. Steinhardt, Proc. Natl. Acad. Sci. USA **106**, 20658 (2009).
[34] D. S. Wiersma, Nat. Photon. **7**, 188 (2013).
[35] L. S. Froufe-Pérez, M. Engel, J. J. Sáenz, and F. Scheffold, Proc. Natl. Acad. Sci. USA **114**, 9570 (2017).
[36] A. L. Gaunt, T. F. Schmidutz, I. Gotlibovych, R. P. Smith, and Z. Hadzibabic, Phys. Rev. Lett. **110**, 200406 (2013).
[37] J. Simon, W. S. Bakr, R. Ma, M. E. Tai, P. M. Preiss, and M. Greiner, Nature (London) **472**, 307 (2011).
[38] H. Shima, T. Nomura, and T. Nakayama, Phys. Rev. B **70**, 075116 (2004).
[39] A. Croy, P. Cain, and M. Schreiber, Eur. Phys. J. B **85**, 165 (2012).
[40] F. M. Izrailev, A. A. Krokhin, and N. Makarov, Phys. Rep. **512**, 125 (2012).
[41] A. Weinrib and B. I. Halperin, Phys. Rev. B **27**, 413 (1983).
[42] H. Rieger and F. Iglói, Phys. Rev. Lett. **83**, 3741 (1999).
[43] J. A. Hoyos, N. Laflorencie, A. d. P. Vieira, and T. Vojta, Europhys. Lett. **93**, 30004 (2011).
[44] C. Chatelain, Phys. Rev. E **89**, 032105 (2014).
[45] M. Pasienski and B. DeMarco, Opt. Express **16**, 2176 (2008).
[46] A. L. Gaunt and Z. Hadzibabic, Sci. Rep. **2**, 721 (2012).
[47] H. Labuhn, D. Barredo, S. Ravets, S. De Léséleuc, T. Macrì, T. Lahaye, and A. Browaeys, Nature (London) **534**, 667 (2016).
[48] P. Schauß, J. Zeiher, T. Fukuhara, S. Hild, M. Cheneau, T. Macrì, T. Pohl, I. Bloch, and C. Groß, Science **347**, 1455 (2015).
[49] S. Nadj-Perge, I. K. Drozdov, J. Li, H. Chen, S. Jeon, J. Seo, A. H. MacDonald, B. A. Bernevig, and A. Yazdani, Science **346**, 602 (2014).
[50] A. Gabrielli and S. Torquato, Phys. Rev. E **70**, 041105 (2004).
[51] E. Chertkov, R. A. DiStasio, Jr., G. Zhang, R. Car, and S. Torquato, Phys. Rev. B **93**, 064201 (2016).
[52] R. D. Batten, F. H. Stillinger, and S. Torquato, J. Appl. Phys. **104**, 033504 (2008).
[53] J. Luck, J. Stat. Phys. **72**, 417 (1993).
[54] E. Fradkin, Phys. Rev. B **33**, 3263 (1986).
[55] R. Nandkishore, D. A. Huse, and S. L. Sondhi, Phys. Rev. B **89**, 245110 (2014).
[56] J. H. Pixley, Y.-Z. Chou, P. Goswami, D. A. Huse, R. Nandkishore, L. Radzihovsky, and S. Das Sarma, Phys. Rev. B **95**, 235101 (2017).
[57] S. V. Syzranov and L. Radzihovsky, Annu. Rev. Condens. Matter Phys. **9**, 35 (2018).
[58] H. Schmidt, Phys. Rev. **105**, 425 (1957).
[59] D. Thouless, J. Phys. C: Solid State Phys. **5**, 77 (1972).
[60] L. G. C. Rego and G. Kirczenow, Phys. Rev. Lett. **81**, 232 (1998).
[61] A. Larkin and Y. N. Ovchinnikov, Zh. Eksp. Teor. Fiz. **55**, 2262 (1968); [Sov. Phys.–JETP **28**, 1200 (1969)].
[62] J. Maldacena, S. H. Shenker, and D. Stanford, J. High Energy Phys. (2016) 106.
[63] T. Platini and D. Karevski, Eur. Phys. J. B **48**, 225 (2005).
[64] C.-J. Lin and O. I. Motrunich, Phys. Rev. B **97**, 144304 (2018).
[65] S. Xu and B. Swingle, arXiv:1802.00801.
[66] V. Khemani, D. A. Huse, and A. Nahum, Phys. Rev. B **98**, 144304 (2018).
[67] M. Fagotti, Phys. Rev. B **96**, 220302(R) (2017).
[68] T. P. Eggarter and R. Riedinger, Phys. Rev. B **18**, 569 (1978).
[69] B. McCoy, Phys. Rev. **188**, 1014 (1969).
[70] S.-k. Ma, C. Dasgupta, and C.-k. Hu, Phys. Rev. Lett. **43**, 1434 (1979).
[71] F. Iglói and I. A. Kovács, Phys. Rev. B **97**, 094205 (2018).
[72] G. Refael and J. E. Moore, Phys. Rev. Lett. **93**, 260602 (2004).
[73] See Supplemental Material at http://link.aps.org/supplemental/10.1103/PhysRevB.100.134206 for additional data showing agreement of $S_\ell$ with the form (16) over a larger range of values of $\alpha$.
[74] R. A. Hyman and K. Yang, Phys. Rev. Lett. **78**, 1783 (1997).
[75] L. Zhang, B. Zhao, T. Devakul, and D. A. Huse, Phys. Rev. B **93**, 224201 (2016).
[76] A. Goremykina, R. Vasseur, and M. Serbyn, Phys. rev. Lett. **122**, 040601 (2019).
[77] O. Motrunich, S.-C. Mau, D. A. Huse, and D. S. Fisher, Phys. Rev. B **61**, 1160 (2000).